

# Artificial Cells, Nanomedicine, and Biotechnology

## An International Journal

ISSN: (Print) (Online) Journal homepage: <https://www.tandfonline.com/loi/ianb20>

## Ultrasound-sensitive cRGD-modified liposomes as a novel drug delivery system

Nour M. AlSawaftah, Vinod Paul, Doua Kosaji, Leen Khabbaz, Nahid S. Awad & Ghaleb A. Hussein

To cite this article: Nour M. AlSawaftah, Vinod Paul, Doua Kosaji, Leen Khabbaz, Nahid S. Awad & Ghaleb A. Hussein (2022) Ultrasound-sensitive cRGD-modified liposomes as a novel drug delivery system, *Artificial Cells, Nanomedicine, and Biotechnology*, 50:1, 111-120, DOI: [10.1080/21691401.2022.2074439](https://doi.org/10.1080/21691401.2022.2074439)

To link to this article: <https://doi.org/10.1080/21691401.2022.2074439>



© 2022 The Author(s). Published by Informa UK Limited, trading as Taylor & Francis Group



Published online: 11 May 2022.



Submit your article to this journal [↗](#)







View related articles [↗](#)



View Crossmark data [↗](#)

## Ultrasound-sensitive cRGD-modified liposomes as a novel drug delivery system

Nour M. AlSawafah<sup>a,b</sup> , Vinod Paul<sup>a,b</sup> , Doua Kosaji<sup>a</sup>, Leen Khabbaz<sup>a</sup>, Nahid S. Awad<sup>a</sup>  and Ghaleb A. Hussein<sup>a,b</sup> 

<sup>a</sup>Department of Chemical Engineering, College of Engineering, American University of Sharjah, Sharjah, United Arab Emirates; <sup>b</sup>Materials Science and Engineering Program, American University of Sharjah, Sharjah, United Arab Emirates

### ABSTRACT

Targeted liposomes enable the delivery of encapsulated chemotherapeutics to tumours by targeting specific receptors overexpressed on the surfaces of cancer cells; this helps in reducing the systemic side effects associated with the cytotoxic agents. Upon reaching the targeted site, these liposomes can be triggered to release their payloads using internal or external triggers. In this study, we investigate the use of low-frequency ultrasound as an external modality to trigger the release of a model drug (calcein) from non-targeted and targeted pegylated liposomes modified with cyclic arginine–glycine–aspartate (cRGD). Liposomes were exposed to sonication at 20-kHz using three different power densities (6.2, 9, and 10 mW/cm<sup>2</sup>). Our results showed that increasing the power density increased calcein release from the sonicated liposomes. Moreover, cRGD conjugation to the surface of the liposomes rendered cRGD-liposomes more susceptible to ultrasound compared to the non-targeted liposomes. cRGD conjugation was also found to increase cellular uptake of calcein by human colorectal carcinoma (HCT116) cells which were further enhanced following sonicating the cells with low-frequency ultrasound (LFUS).

### ARTICLE HISTORY

Received 8 January 2022  
Revised 28 March 2022  
Accepted 30 April 2022

### KEYWORDS

Cancer; liposomes; cRGD; ultrasound; calcein

### Introduction

Cancer nanotherapeutics have attracted a great deal of attention in the recent decade because of their ability to overcome several limitations of conventional therapies, such as poor specificity, high toxicity, poor water solubility, adverse systemic side effects, induction of drug resistance, and limited bioavailability [1–3]. Several cancer nanotherapeutics have been developed, including carbon nanotubes (CNTs), polymeric micelles, dendrimers, solid lipid NPs, quantum dots (QDs), gold NPs, and liposomes. Liposomes are considered the most successful nanocarriers developed for drug delivery applications due to their versatile structure, biocompatibility, biodegradability, low toxicity, and non-immunogenicity [4,5]. Liposomes are composed of phospholipid bilayers arranged in concentric spheres around an aqueous core. These phospholipid bilayers assume such an arrangement so that the hydrophobic tails are facing away from the aqueous environment. In contrast, the hydrophilic heads face the external aqueous environment and aqueous core [6–8]. Their amphiphilic nature allows them to entrap both hydrophilic and hydrophobic drugs. Coating the liposomes with a hydrophilic polymer, such as polyethylene glycol or (PEG), forms “PEGylated” or “stealth” liposomes with increased repulsive forces between the liposomes and serum-proteins including opsonin, thus, increasing their circulation time in the blood [10]. Stealth liposomes can passively target the tumour tissues through

abnormal wide fenestrations, leakiness, and the lack of lymphatic drainage of tumour endothelial cells to extravasate into tumours. This is known as the enhanced permeability and retention (EPR) effect [9]. The downside of passive targeting is that it lacks specificity and selectivity. To address this issue, the surface of the stealth liposomal can be functionalized using different moieties (ligands) to improve their targeting specificity and the subsequent cellular internalization [4,10]. Different ligands have been used, such as proteins, peptides, aptamers, carbohydrates, and antibodies [11–14].

Currently, a class of proteins referred to as the integrin family is being intensively researched for targeted therapy. Integrins are heterodimeric transmembrane glycoproteins comprised of an  $\alpha$  and a  $\beta$  subunit. There are 24 known integrin heterodimers made up of 18  $\alpha$  and 8  $\beta$  subunits [15]. Integrins play a vital role in cell adhesion, motility, signalling, and survival because they bind to various components of the extracellular matrix (ECM) [15,16]. As far as cancer is concerned, integrins were found to play important roles in cancer progression, neoangiogenesis, and some subtypes have been described to be upregulated on many cancer cells, namely  $\alpha_v\beta_3$ ,  $\alpha_v\beta_5$ , and  $\alpha_5\beta_1$  [15,17]. The overexpression of certain integrins on cancer cells can be attributed to the need to meet the elevated demand for nutrients and oxygen needed to maintain the rapid growth of tumours.

Arginine-glycine-aspartic acid (RGD), is a polypeptide that plays a vital role in cell adhesion, cellular differentiation,

migration, and attachment to the extracellular matrix (ECM). RGD peptides have linear and cyclic structures. However, the steric hindrance of the structure of the cyclic RGD (cRGD) makes them resist proteolysis and have the ability to bind with higher affinities to integrin receptors compared to linear RGD peptides. Moreover, RGD has a relatively high and specific affinity towards  $\alpha_v\beta_3$  integrins over-expressed in tumour neovasculature. Previous studies have shown that liposomes conjugation to RGD peptides has great potential for cancer therapy [18–20]. To trigger the release of therapeutic agents from liposomes, ultrasound is emerging as a promising mechanism for spatiotemporal drug release from drug-loaded liposomes. The effects of ultrasound as a triggering mechanism can be divided into thermal effects due to the increase in the medium's temperature as energy is absorbed, and mechanical effects due to acoustic cavitation. Acoustic cavitation is the formation, growth, and collapse of bubbles in a medium due to pressure changes. Stable cavitation is when the bubble's radius varies about an equilibrium value, while inertial (transient) cavitation is when the bubbles grow rapidly, expanding to 2- or 3-fold their resonant size and then collapse violently [21–23]. The occurrence of cavitation depends on the frequency and intensity of ultrasound, as well as the availability and number of cavitation nuclei.

Here, we describe the synthesis of pegylated (stealth) liposomes loaded with the model drug calcein and conjugated to cRGD (targeted liposomes). The ability of cRGD liposomes to target  $\alpha_v\beta_3$  receptors overexpressed on the surface of human colorectal carcinoma (HCT116) cells will be examined as well as the effect of applying low-frequency ultrasound (LFUS) in triggering drug release and enhancing cellular uptake of drugs from targeted and non-targeted liposomes.

## Materials and methods

### Materials

1,2-distearoyl-sn-glycero-3-phosphoethanolamine-*N*-[amino (polyethylene glycol)-2000] (ammonium salt) (DSPE-PEG(200)-NH<sub>2</sub>) and 1,2-dipalmitoyl-sn-glycero-3-phosphocholine (DPPC) were obtained from Avanti Polar Lipids Inc. (Alabaster, Alabama, USA, supplied by Labco LLC, Dubai, UAE). Cyanuric

chloride, L-glutamine, antibiotic solutions, trypsin, cholesterol, calcein disodium salt, the protein assay kit (bicinchoninic acid), RPMI-1640 media, foetal bovine serum as well as Dulbecco's phosphate buffered saline (DPBS) were obtained from Sigma-Aldrich Chemie GmbH (supplied by Labco LLC, Dubai, UAE). Cyclic (Arg-Gly-Asp-d-Phe-Cys) (cRGD) was purchased from Musechem (Fairfield, NJ, USA, supplied by Labco LLC, Dubai, UAE). Chloroform was purchased from Panreac Quimica S.A. (Barcelona, Spain). The human colorectal carcinoma (HCT116) cell line was obtained from the European Collection of Authenticated Cell Cultures (ECACC general cell collection, Salisbury, UK). Figure 1 shows the difference in structure between the linear and cyclic RGD.

### Preparation of liposomes

The thin-film hydration method was used to prepare the liposomes [24]. DPPC, DSPE-PEG(2000)-NH<sub>2</sub>, and cholesterol were added to a round-bottom flask at molar ratios of 65:5:30, respectively. Chloroform (4 ml) was then added to dissolve the lipids and evaporated while rotating under a vacuum at 50 °C for 20 min. A lipid film was formed, and 2 ml of the calcein, dissolved in PBS buffer (30 mM), was added to hydrate the lipid film using the rotatory evaporator. Unilamellar liposomes were formed using a sonicating bath (35 kHz) for 2 min (Elma D-78224, Melrose Park, Illinois, USA). The liposomes were then extruded using an extruder containing 200-nm polycarbonate filters (Avanti Polar Lipids, Inc., Alabaster, AL, USA). Unencapsulated calcein was removed by passing the liposomes through a gel filtration medium (Sephadex G-100). cRGD was conjugated to the liposomes using cyanuric chloride (2,4,6 trichloro-1,3,5 triazine) as a coupling agent, 10 mg of cyanuric chloride were dissolved in 500  $\mu$ l of acetone and 1 ml of deionized water. It was added to the liposomes in a 1:1 molar ratio (cRGD: DSPE-PEG(2000)-NH<sub>2</sub>). The reaction was left to stir for 3 h at 2 °C. Three hundred and forty-six microlitres of the cRGD solution (5 mg of cRGD dissolved in 1 ml of borate buffer at pH~8.5) were added to the mixture and were left stirring overnight. The preferential order for incorporating nucleophiles in cyanuric chloride was found to be alcohol > thiol > amine [25]. The expected

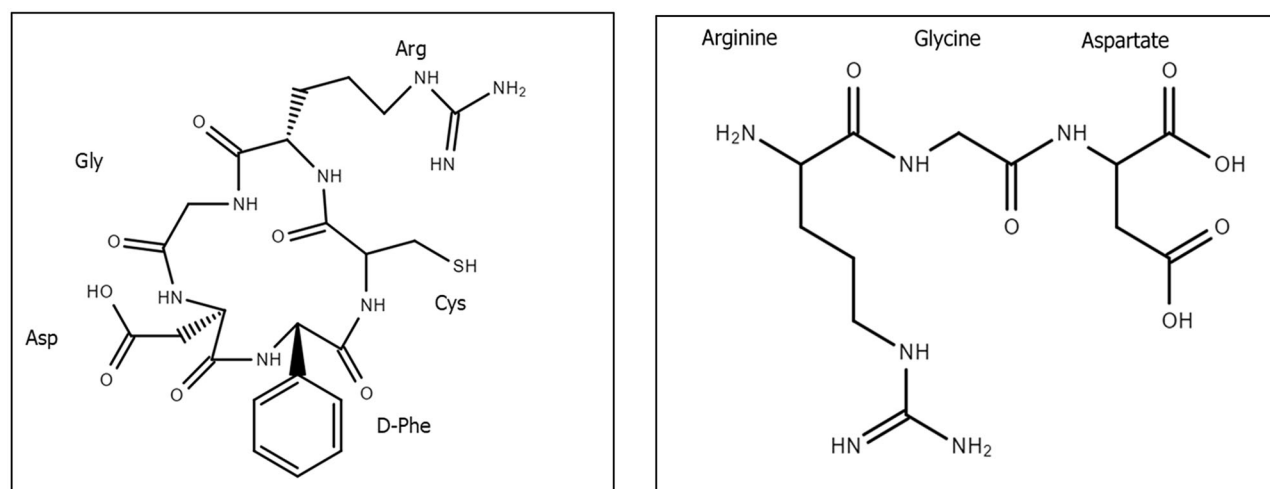
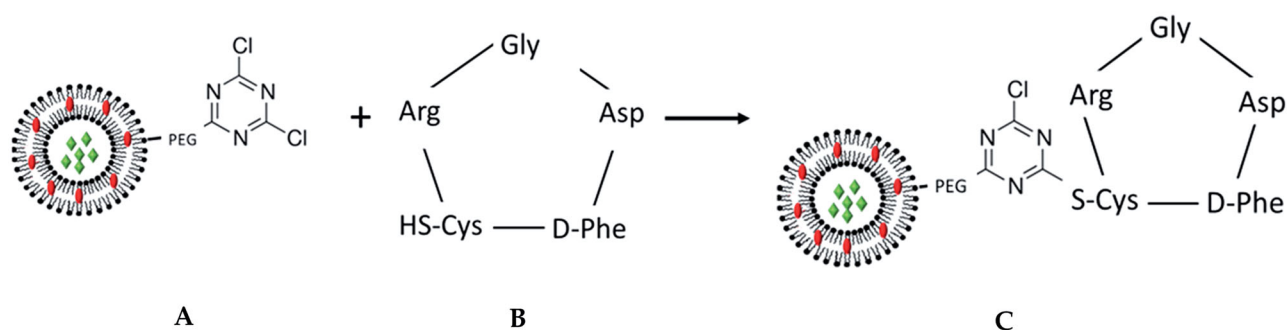


Figure 1. Chemical structure of linear RGD (right), and cyclic RGD (Arg-Gly-Asp-D-Phe-Cys) (left).



**Figure 2.** cRGD conjugation to liposomes using cyanuric chloride as a coupling agent. Pegylated liposomes binds to cyanuric chloride (A), cRGD molecule is added (B), cRGD is conjugated to the pegylated liposomes (C).

coupling reaction is shown in Figure 2. The same volume of cyanuric chloride was added to the control and conjugated liposomes. The only difference is that the cRGD solution (prepared in borate buffer) was not added to the control liposomes. Instead, the same volume of pure borate buffer was added to the control liposomes. Both types of liposomes were then incubated under the same reaction conditions. Finally, gel filtration removed unconjugated cRGD, and the collected fractions were stored at 4 °C until further use.

### Liposomes' characterization

The hydrodynamic radius of the prepared liposomes was measured using a dynamic light scattering (DLS) machine (DynaPro<sup>®</sup> NanoStar<sup>™</sup>, Wyatt Technology Corp., Santa Barbara, California, USA). Fifteen microlitres of the liposomes were diluted with 1 ml of PBS buffer, and the measurements were taken at room temperature (three replicates from each sample). The Stewart assay was used for phospholipids quantification [26], and 50  $\mu$ l of the liposomes was dried using a rotatory evaporate (50 °C with vacuum). The dried lipids were dissolved in chloroform (1 ml) and were placed in a sonicating bath (35 kHz) at 25 °C for 10 min (Elma D-78224, Melrose Park, Illinois, USA). Different volumes of the disrupted liposomes were placed in centrifuge tubes. The volume in each tube was topped up to 2 ml with chloroform. Ammonium ferrothiocyanate was also added to each tube (2 ml) which was then vortexed for 20 s before centrifugation for 10 min at 1000 rpm. The bottom chloroform layer was transferred into a cuvette and the optical density was measured using ultraviolet-visible (UV-vis) spectroscopy at  $A_{\max} = 485$  nm. The total concentration of the phospholipids present in the liposomes was calculated using a standard calibration curve of DPPC using three replicates for each sample.

cRGD conjugation was verified using the Bicinchoninic Acid Assay (BCA) prepared by mixing the QuantiPro QA buffer, QuantiPro QB, and  $\text{CuSO}_4$  in a ratio of 25:25:1, respectively. Four hundred microlitres of the liposomes were added into an Eppendorf tube and the volume was completed to 1 ml with PBS buffer. One millilitre of the prepared BCA reagent was then added and the samples were incubated for 1 h at 60 °C. The optical density of the samples was determined using UV-vis spectroscopy at  $A_{\max} = 562$  nm (three replicates for each sample) [27]. cRGD concentration was calculated using a standard calibration curve prepared using known concentrations of cRGD.

TEM imaging was performed by placing 3  $\mu$ l of the liposomal solution on a plasma thin holey carbon 400-mesh copper grid. This was followed by the removal of the excess solution by filter paper blotting. The surface of the grid was cleaned by gentle touching with a Parafilm containing deionized water (30  $\mu$ l), this was then followed by filter paper blotting, and both steps were repeated twice. The grid was then placed facing down on a 20  $\mu$ l drop of uranyl acetate substitute solution (1% w/v) for 30 s and the access stain was removed. The sample was then air-dried at room temperature. The images were obtained using FEI Talos F200X transmission electron microscope (Thermo Fisher Scientific, USA).

The amount of the calcein loaded inside the control and cRGD liposomes were calculated as described by Ishii and Nagasaka [28]. The filtered liposomes were diluted ( $\times 40$ ) using PBS buffer, and their fluorescence values were recorded before and after the addition of Triton X-100 using QuantaMaster QM 30 Spectrofluorometer (Photon Technology International, Edison NJ, USA) with excitation and emission wavelengths of 495 and 515 nm, respectively. The concentration of the encapsulated calcein was determined using a calibration curve of calcein showing the fluorescence intensity against different concentrations of calcein dissolved in PBS buffer. The serial dilutions were prepared while maintaining a constant liquid volume in the cuvette (366 nM to 3 mM). The calibration curve showed that calcein fluorescence value increased with the increase in concentration up to 0.012 mM. Then, the fluorescence intensity decreased with the increase in calcein concentration due to calcein self-quenching properties.

### Low-frequency ultrasound release studies (online experiments)

Liposomes (75  $\mu$ l) were placed in a cuvette and were diluted with 3 ml PBS [29]. Calcein release from the liposomes was monitored online during the sonication of the samples using a 20-kHz ultrasound probe (VCX750, Sonics & Materials Inc., Newtown, CT, USA). Changes in calcein fluorescence were monitored online using a spectrofluorometer (QuantaMaster QM, Photon Technology International, NJ, USA) using an excitation wavelength of 495 nm and an emission wavelength of 515 nm. Three different power densities were investigated (6.2, 9, and 10  $\text{mW}/\text{cm}^2$ ). The fluorescence intensity of calcein without sonication was recorded for 1 min and represented the baseline ( $I_0$ ); pulses of LFUS were then applied (20 s on and 20 s off). The pulses were stopped when calcein

fluorescence reached a plateau. Next, Triton X-100, a surfactant, was added to lyse the liposomes releasing all of the remaining encapsulated calceins. All the intensities recorded online were used to calculate the cumulative fraction released (CFR) using the following equation [27]:

$$CFR = \frac{I_t - I_0}{I_\infty - I_0} \quad (1)$$

Where  $I_0$  represents the baseline intensity,  $I_t$  represents the intensity at time  $t$ , and  $I_\infty$  represents the highest fluorescence intensity value obtained (after the addition of the Triton X-100 surfactant).

### Flow cytometry studies

Human colorectal carcinoma (HCT116) cells were cultured at a density of  $2 \times 10^5$  cells/ml in 6-well plates. After a 24-h incubation, the cells were treated with the control (non-targeted) liposomes and cRGD-liposomes followed by further incubation for 1 h. Plates exposed to LFUS (35 kHz) were placed in a sonicating bath ( $1 \text{ W/cm}^3$ ) for 5 min. The plates were incubated for 1.5 h at  $37^\circ\text{C}$  and 5%  $\text{CO}_2$  [30]. The cells were washed using PBS buffer and were then harvested with trypsin solution. Cellular uptake of calcein was measured using flow cytometry [FC 500 (Beckman Coulter FC 500), Brea, CA, USA]. Three independent assays were performed for each treatment. The viability of the cells exposed to LFUS was determined using the Trypan Blue exclusion assay.

### Determination of cell viability

Human colorectal carcinoma cells (HCT116) were seeded in a 6-well plate ( $6 \times 10^5$  cells/well) and incubated overnight. Next, the media was replaced and the plates were exposed to sonication using an LFUS (35 kHz) sonicating bath. The plates were then incubated for a further 2 h. The cells were then detached using Trypsin EDTA and the percentage of cell viability was recorded using the Trypan Blue dye exclusion method.

### Imaging of cellular uptake of calcein using a fluorescent microscope

HCT116 cells ( $2 \times 10^5$  cells/ml) were seeded in 6-well plates for 24 h and incubated for a further 2 h with either control or cRGD liposomes. Sonicated plates were placed in a sonicating bath (35 kHz) for 5 min. The media was removed from the wells, and the cells were washed with PBS before being fixed with 4% Formaldehyde. Further washing was carried out using a PBS buffer before imaging. The plates were then examined using a fluorescent microscope (Olympus IX53, excitation filter at 470–495 nm, and emissions at 510–550 nm).

### Statistical analysis

All the results reported here are the average  $\pm$  standard deviation (SD). Two-tailed  $t$ -tests were used to determine the statistical significance of the results;  $p$ -value  $< .05$  was considered statistically significant.

**Table 1.** Summary of the hydrodynamic radius and percentage polydispersity (%Pd) of the prepared liposomes.

	Radius (nm)	%Pd
Control liposomes	$84.98 \pm 0.23$	$12.88 \pm 0.37$
cRGD liposomes	$99.36 \pm 10.66$	$18.58 \pm 5.93$

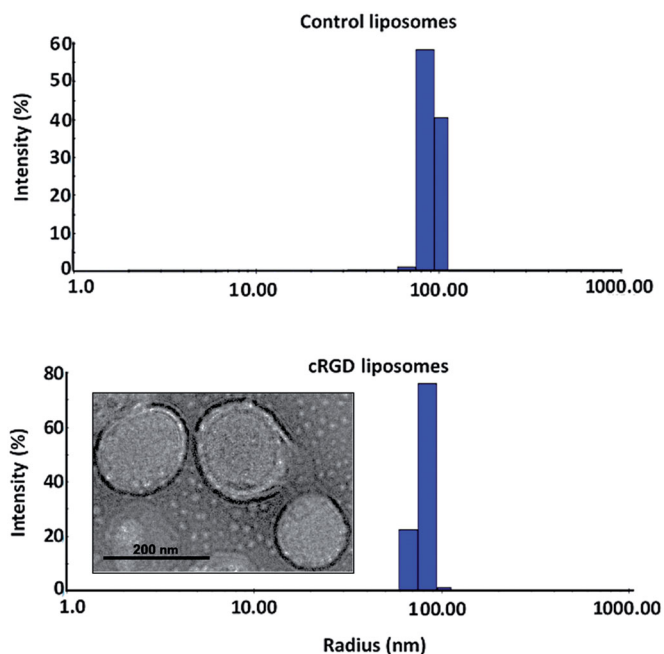


**Figure 3.** Size distribution of the control and cRGD liposomes together with TEM images of the cRGD liposomes.

## Results

### Characterization of liposomal formulations

The measured sizes and polydispersity (%Pd) of the prepared liposomes are summarized in Table 1 below. The two-tailed  $t$ -test analysis yielded a  $p$ -value of  $1 \times 10^{-5}$  indicating that the targeted cRGD liposomes are statistically larger compared to the control (non-targeted) liposomes. The Stewart assay confirmed that both the control and cRGD liposomes had a similar concentration of lipids ( $6.02 \pm 2.06$  and  $5.41 \pm 1.83$  mg/mL, respectively,  $p = .68$ ). In addition, cRGD liposomes showed approximately a 2-fold increase in protein content compared to non-targeted liposomes ( $0.014851 \pm 0.000762$   $\mu\text{g/mL}$  for the control liposomes and  $0.054419 \pm 0.014697$   $\mu\text{g/mL}$  for the cRGD liposomes ( $p = .009611$ ). Figure 3 shows the size distribution of both types of liposomes and a TEM image of cRGD liposomes.

The quantification of the encapsulated calcein inside both the control and cRGD liposomes showed that both types of liposomes encapsulated  $1 \text{ mM} \pm 0.1$  of calcein inside their cores. cRGD was conjugated to the liposomes after being prepared and loaded with calcein (post-insertion). Therefore, the conjugation process had no effect on the amount of loaded calcein. A calibration curve of calcein fluorescence against concentration showed that at the concentration of 1 mM, calcein is self-quenched with no fluorescence properties. Thus, when entrapped inside the liposomes at this concentration, calcein is self-quenched, which justifies using it as the baseline. As calcein is released from the liposomes,



self-quenching is reduced, and the fluorescence readings will increase as the calcein is released from our liposomes.

### Stability of the control and targeted liposomes

To examine the stability of both the prepared liposomes in terms of maintaining their structure and the ability to retain their load, the size of the liposomes was measured following their incubation for 24 h at 37 °C in FBS (10%), and the measurements showed no significant change in the hydrodynamic radii of both the control ( $85.36 \pm 1.43$ ,  $p = .698$ ) and cRGD liposomes ( $98 \pm 7.51$ ,  $p = .872$ ). In addition, calcein encapsulation efficiency was estimated using a spectrofluorometer and the results showed that both the control and cRGD liposomes were fairly stable, releasing on average 17 and 14% of the encapsulated calcein, respectively, after 24 h of incubation (no ultrasound) at 37 °C.

### Low-frequency ultrasound-triggered release

Calcein release from both control and cRGD liposomes was triggered using LFUS delivered to the sonicated samples through a 20-kHz probe at different power densities (6.2, 9, and 10 mW/cm<sup>2</sup>). The released calcein was recorded through the changes in calcein fluorescence intensity. The normalized-average release profiles for both the control and cRGD liposomes are shown in Figure 4. Upon applying pulsed LFUS, the fluorescence intensity of the released calcein showed an increase, indicating that calcein release from liposomes was triggered when LFUS was applied. Moreover, calcein release from both the control and cRGD liposomes increased with the increase in the power density. Finally, the addition of the surfactant (i.e. Triton X-100) lysed the liposomes, releasing the remaining load of calcein. This slightly increased fluorescence measurements, indicating that most of the encapsulated calcein was already released following 250 s of pulsed sonication. Overall, cRGD liposomes were more sensitive to ultrasound, releasing more calcein compared to the control liposomes at all the power densities used.

A detailed comparison between the first three pulses at each power density in terms of the cumulative fraction release (CFR) is shown in Figure 5. The two-tailed *t*-test results show that the percentage release after the first pulse increases significantly ( $p < .05$ ) as the power density increases for both the control and cRGD liposomes. In addition, cRGD liposomes clearly show higher release compared to release from control non-targeted liposomes at each tested power density.

The mechanical index (MI) is a parameter used to indicate an ultrasound beam's ability to cause cavitation and is mathematically represented by Equation (2).

$$MI = \frac{P_{neg}}{\sqrt{f}} \quad (2)$$

$$P_{neg} = \sqrt{2} Z I \quad (3)$$

Here,  $P_{neg}$  represents the peak-negative pressure (expressed in units of MPa) which is dependent upon the acoustic impedance of water,  $Z$  (for human soft tissues, the

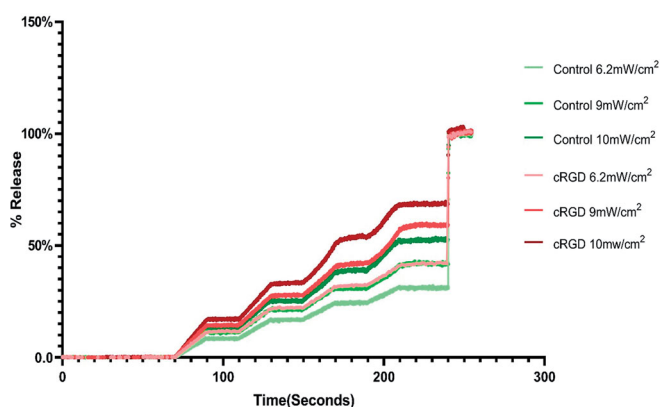


Figure 4. Normalized-averaged release profiles of three batches of calcein loaded cRGD liposomes and non-targeted (control) liposomes.

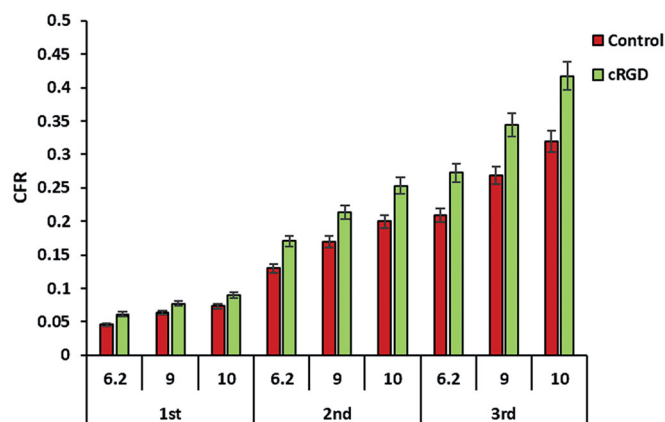


Figure 5. Comparison of calcein release from the control and cRGD liposomes following the exposure to the first three pulses of ultrasound using three different power densities and expressed in terms of CFR.

values of  $Z$  are comparable to those of water), and the intensity of the LFUS denoted by  $I$ . Mathematically, peak-negative pressure is calculated using Equation (3) [31].

The acoustic impedance of water has a value of 1.48 MPas/m [32,33], and the LFUS power densities used in this research were 6.2, 9, and 10 mW/cm<sup>2</sup>. Using Equation (2), the MI values were calculated as 0.096, 0.115, and 0.121, respectively, which are well below the collapse cavitation threshold of 0.3.

### Cellular uptake of calcein loaded inside the liposomes

Flow cytometry analysis was carried out to determine calcein uptake by the human colorectal carcinoma cell line (HCT116) incubated for 1 h with either the control or cRGD liposomes. As seen in Figure 6, the geometric means of the cellular internalization of calcein showed higher uptake of calcein from cRGD liposomes ( $111,920 \pm 31,750$ ) compared to the uptake from the control liposomes ( $3120 \pm 347$ ). Moreover, sonicating the cells with LFUS at 35 kHz (1 W/cm<sup>2</sup>) for 5 min resulted in a further enhancement of calcein uptake by the cells, as evidenced by a mean fluorescence value of the control liposomes ( $4840 \pm 394$ ) vs. cRGD liposomes ( $141,380 \pm 4890$ ). These results show that applying LFUS alone increased the calcein uptake of the control liposomes by 1.5-fold, cRGD conjugation increased calcein uptake by 35-fold compared to the control liposomes.

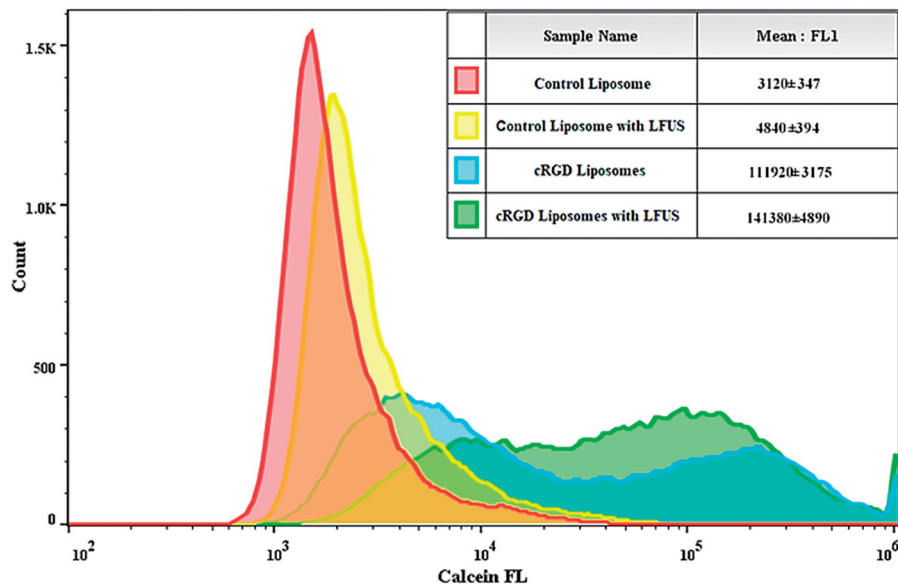


**Figure 6.** Calcein uptake by HCT116 cell line incubated with either the control or cRGD liposomes and sonicated with ultrasound (US). Results are the average of three batches of liposomes.

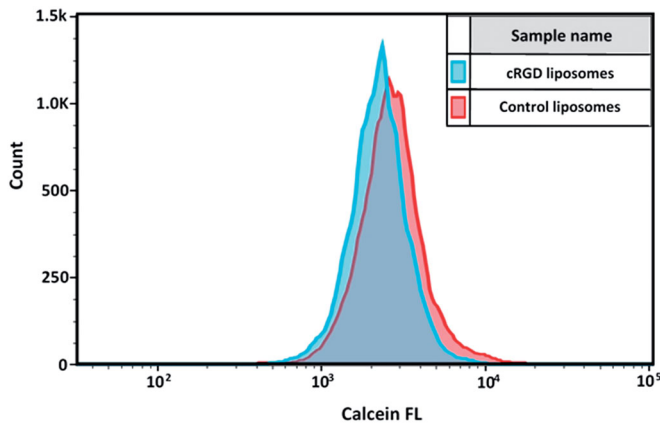


**Figure 7.** Calcein uptake by MCF-7 cell line incubated with either the control or cRGD liposomes.

Combining cRGD liposomes with LFUS showed a 45-fold increase in calcein uptake compared to the uptake from control liposomes and 29-fold increase compared to the uptake from the control liposomes triggered with LFUS.

To prove that the enhanced calcein uptake from the targeted liposomes is due to the overexpression of  $\alpha_v\beta_3$  receptors, an  $\alpha_v\beta_3$ -negative cell line (MCF-7) was used as a negative control. No significant difference in cellular uptake of calcein following the incubation of MCF-7 cells with both the control and cRGD liposomes was recorded, with fluorescence intensities of  $2500 \pm 286$  AU and  $2000 \pm 173$ , respectively ( $p = .621$ ) (Figure 7).

To prove that the enhanced calcein uptake from the targeted liposomes is due to the overexpression of  $\alpha_v\beta_3$  receptors, an  $\alpha_v\beta_3$ -negative cell line (MCF-7) was used as a negative control. No significant difference in cellular uptake of calcein following the incubation of MCF-7 cells with both the control and cRGD liposomes was recorded, with fluorescence intensities of  $2500 \pm 286$  AU and  $2000 \pm 173$ , respectively ( $p = .621$ ) (Figure 7).

Applying LFUS (at 35 kHz) had no effect on the viability of the human colorectal carcinoma cells (HCT116), as shown in Table 2, where no significant difference in the percentage of viable cells before and after sonication with ultrasound is observed.

### Imaging of cellular uptake of calcein using a fluorescent microscope

To better visualize the cellular uptake of calcein from the control and cRGD liposomes by the HCT116 cells, fluorescent microscopic images of the cells were taken after an hour of incubation with the liposomes. As shown in Figure 8, the images showed that cells incubated with cRGD liposomes showed a higher fluorescence intensity of calcein with more calcein present inside the cytoplasm of the cell compared to the cells incubated with the control liposomes, which showed a lower fluorescence signal. These findings support the flow cytometry analysis results and suggest a higher uptake of calcein from cRGD liposomes compared to the control liposomes.

### Discussion

The present study suggests that combining targeted liposomes with LFUS is an effective mechanism for the controlled release of drugs from the liposomes and the enhanced drug uptake by the cancer cells. We have successfully synthesized targeted liposomes with cRGD conjugated to their surfaces through the use of cyanuric chloride, which is a chemoselective linker with thermally controlled reactivity due to the presence of three electrophilic carbons. cRGD has a high affinity for  $\alpha_v\beta_3$ . It was previously confirmed that the human colorectal carcinoma (HCT116) cell lines are enriched with  $\beta_3$  integrins acting as a specific recognition site of ligands targeting  $\beta_3$  [34]. Thus, cRGD was conjugated to the liposomes to synthesize a nano-sized HCT116-targeting delivery system.

Our results showed that despite a significant increase ( $p \leq .05$ ) in liposomal size following cRGD conjugation, both non-targeted and cRGD liposomes were found to fall within the size range of small lamellar vesicles (SLVs) and the optimal size range to take advantage of the EPR effect (diameter  $< 200$  nm). Moreover, both types of liposomes showed acceptable polydispersity values ( $< 20\%$ ) and both were stable when incubated at  $37^\circ\text{C}$  for 24 h in terms of maintaining their size and retaining their calcein load. This indicates that cRGD conjugation had no adverse effect on liposomal stability.

Liposomes' exposure to pulsed LFUS triggered calcein release from both the control and cRGD liposomes. This is in agreement with previous studies, which showed that sonication triggers drug release from the liposomes [21,27,35–38]. Although the thermal effects produced by ultrasound waves

could play a role in triggering calcein release, we have recorded a small increase in temperature (from  $25$  to  $31^\circ\text{C}$ ) following the first three pulses of ultrasound at the highest power density ( $10\text{ mW}/\text{cm}^3$ ), which is still below the transition temperature of the DPPC, the main component of the liposomes used here (i.e.  $41.3^\circ\text{C}$ ). Heating both the control and cRGD liposomes to  $31^\circ\text{C}$ , without sonication, released  $< 2\%$  of the encapsulated calcein from both types of liposomes. Thus, despite a possible thermal effect, it is likely that cavitation events produced by the ultrasound wave play a major role in triggering the release. Calcein release from targeted and non-targeted liposomes increased with the increasing power density. Both stable and collapsed (inertial) cavitation could have played a role in triggering calcein release [39–41]. According to the literature, the threshold of collapse cavitation is expected to occur at around  $MI = 0.3$  and biological effects are observed at  $MI > 0.7$ , while tissue damage is expected to occur at  $MI > 1.9$  [31,42–44]. The calculated  $MI$  values produced by the three power densities used here were  $0.096$ ,  $0.115$ , and  $0.121$ —all three are below the collapse cavitation threshold of  $0.3$ . This indicates that

**Table 2.** Cell viability following sonication with LFUS (35 kHz) for 5 min.

	Control	Sonicated	<i>p</i> -Value
Viability %	96.9%	97.74%	.862
Std. Dev.	2.45	1.28	

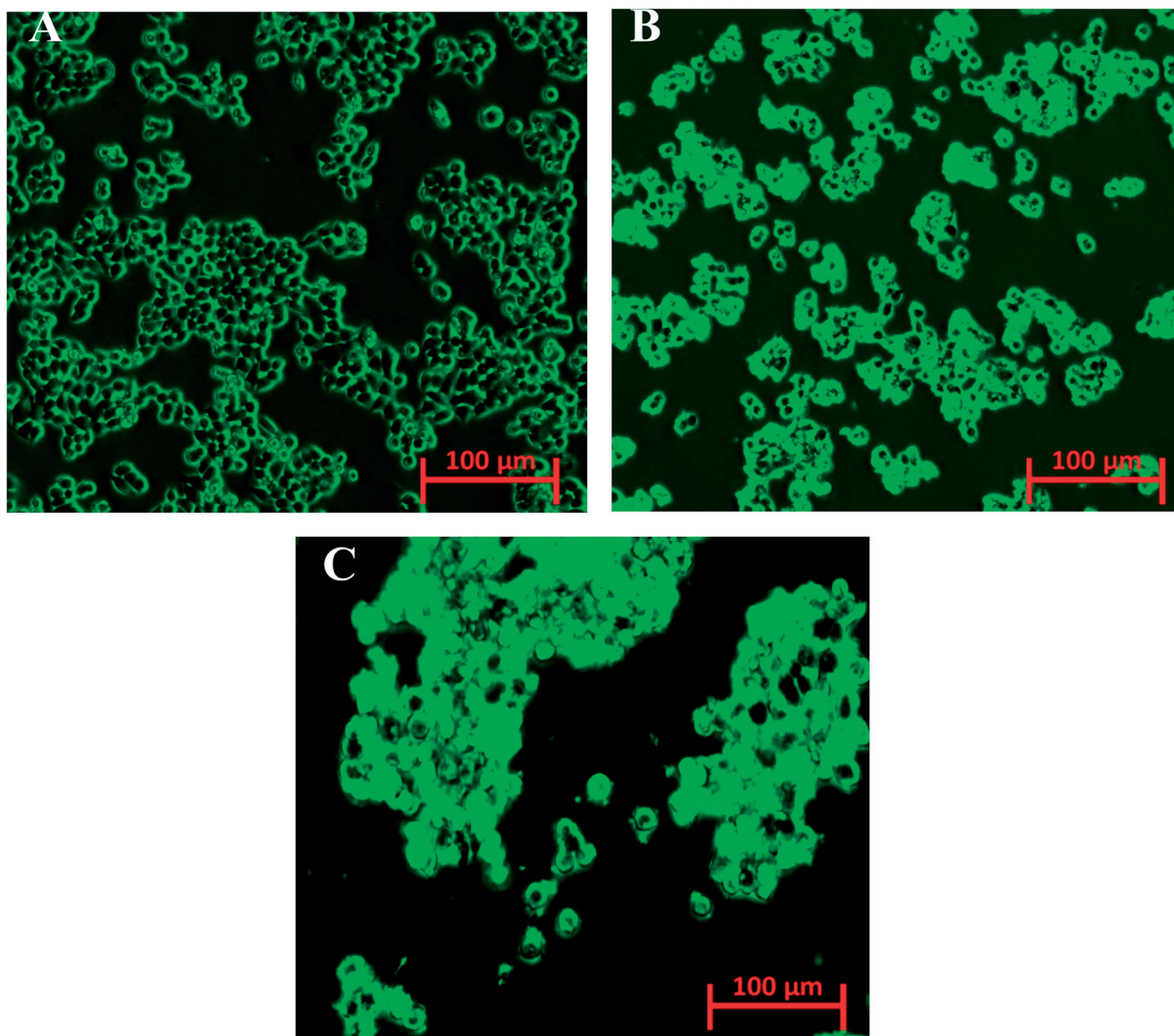


**Figure 8.** Fluorescence microscopic images of HCT116 cells following the incubation with calcein-loaded control liposomes (A), cRGD liposomes (B), cRGD liposomes and sonication with LFUS (at 35 kHz) for 5 min (C).



stable cavitation is likely to be the driving force behind the observed calcein release.

Acoustic cavitation is known to induce pore formation on cellular membranes, a phenomenon known as sonoporation [45]. Both stable and transient/collapse cavitation can cause sonoporation by temporarily affecting the integrity of their phospholipid bilayer and altering membrane permeability. Similar to the cells in our bodies, liposomes are also surrounded by phospholipid bilayer membranes. Therefore, sonication with ultrasound results in increasing their permeability and enhancing the release of the encapsulated calcein in a controlled manner [46]. The formed pores reseal once ultrasound's radiation ceases. This explains why calcein release stopped during the "off" cycle of the pulsed LFUS. Interestingly, cRGD conjugation to the surface of the liposomes rendered these nanovehicles more sensitive to acoustic waves. We have previously shown that the pegylation of the liposomes increases their sonosensitivity; we have previously shown that the pegylation of the liposomes increases their sonosensitivity. Additionally, we have also that the conjugation of targeting moieties (estrone, albumin, transferrin, and Trastuzumab) to pegylated liposomes further increased their sensitivity to LFUS-triggered drug release [27,37,47]. However, in a previous publication, we have also reported that the conjugation of linear RGD to pegylated liposomes had no effect on measured release [27]. The only difference between the two molecules is their molecular weight. cRGD has a higher molecular weight (612.7 g/mol) compared to linear RGD (346.34 g/mol). More studies are needed to understand the mechanism behind this enhanced liposome's sonosensitivity following the conjugation of cRGD to stealth liposomes.

Calcein encapsulation inside the liposomes was already found to enhance calcein uptake by the cancer cells [48]. Here, we compared cellular uptake of calcein and found that more calcein was taken up by the cells from cRGD liposomes compared to the non-targeted control liposomes. This could be due to the difference in the cellular uptake of the liposomal nanocarriers. The similarity between cellular and liposomal membranes (i.e. the phospholipid bilayer) may imply that liposomes can fuse with cellular membranes transferring their load into the cells once both members come in contact. This explains the calcein fluorescent signal when cells were incubated with the control liposomes (Figure 6). However, the fusion process is relatively slow and gradual with time [49]. cRGD liposomes, on the other hand, are able to deliver their load of calcein through both membrane fusion as well as through receptor-moiety binding and receptor-mediated endocytosis. This allows more calcein to be delivered to the cells in a short period of time. Endocytic recycling can be relatively fast ( $t_{1/2} = 1-5$  min) [50], which is reflected by a higher cellular internalization of calcein (Figure 7) and a higher calcein fluorescence intensity inside the cytoplasm of the cells (Figure 8). Previous studies have shown that liposomes conjugated to cRGD showed higher accumulation and higher antitumor activity compared to the non-targeted liposomes when used to target different types of cancer cells with high expression of  $\alpha_v\beta_3$  integrins [34,51-53].

Sonication with LFUS results in the cavitation-mediated pore formation or the sonoporation effect on both the liposomes

and cellular membranes. This enhances cellular uptake of the liposomes and calcein release, resulting in the higher cellular uptake of the agent and enhancing its fluorescence intensity inside the cells, as shown in Figures 6 and 7. These findings suggest that combining targeted liposomes with LFUS results in better control of drug release and drug uptake by the cells, further enhancing their therapeutic efficiency. Sonication of the cells with LFUS had no adverse effects on the cells (as shown in Table 2). This is in agreement with previous studies that showed that irradiation with LFUS did not affect the viability of the cells [54,55]. Thus, the use of LFUS as a trigger of drug release from liposomes is an effective and safe modality.

## Conclusion

This work focussed on the synthesis of cRGD liposomes encapsulating the model drug calcein and the effect of LFUS on controlling payload release. cRGD conjugation enhanced the liposomes' sensitivity to ultrasound and the triggered release increased as the power density increased. cRGD conjugation also enhanced the cellular uptake of calcein by the human colorectal carcinoma (HCT116) cells which were further enhanced following sonicating the cells with LFUS. Our findings suggest that combining targeted liposomes with LFUS is an effective mechanism for the delivery and spatiotemporal controlled release of drugs inside tumours. By utilizing the three types of targeting, namely passive (using size), ligand or active (using cRGD), and triggered (using ultrasound), we envision a comprehensive multimodal drug delivery system to treat cancer.

## Acknowledgments

The authors would like to acknowledge the financial support of the American University of Sharjah Faculty Research Grants, the Al-Jalila Foundation [AJF 2015555], the Al Qasimi Foundation, the Patient's Friends Committee-Sharjah, the Biosciences and Bioengineering Research Institute [BBRI18-CEN-11], GCC Co-Fund Program [IRF17-003], the Takamol Program [POC-00028-18], the Technology Innovation Pioneer (TIP) Healthcare Awards, Sheikh Hamdan Award for Medical Sciences [MRG-57-2019-2020], and the Dana Gas Endowed Chair for Chemical Engineering. We also would like to acknowledge student funding from the Material Science and Engineering Ph.D. program at AUS.

## Author contributions

N.M.A., V.P., D.K., L.K., N.S.A., and G.A.H. designed the study and conducted the analysis. N.M.A., V.P., and N.S.A. drafted the manuscript. G.A.H. revised and edited the manuscript. All authors approved the final version of the manuscript.

## Disclosure statement

The authors declare no conflict of interest.

## Funding

This research was funded by the American University of Sharjah Faculty Research Grants [FRG20-L-E48 and eFRG18-BBRCEN-03], Sheikh Hamdan Award for Medical Sciences [Grant Number: MRG-57-2019-2020], and Friends of Cancer Patients (FoCP). The work in this paper was supported, in part, by the Open Access Program from the American University of

Sharjah [grant number: OAPCEN-1410-E00037]. We also acknowledge the TEM facility of the Core Technology Platform Resources at New York University Abu Dhabi, for their help with the TEM imaging. This paper represents the opinions of the author(s) and does not mean to represent the position or opinions of the American University of Sharjah.

## ORCID

Nour M. AlSawafah  <http://orcid.org/0000-0002-7115-3667>

Vinod Paul  <http://orcid.org/0000-0001-9740-1000>

Nahid S. Awad  <http://orcid.org/0000-0003-0881-4300>

Ghaleb A. Husseini  <http://orcid.org/0000-0002-7244-3105>

## Data availability statement

The data that support the findings of this study are available from the corresponding author, G.A.H., upon reasonable request.

## References

- [1] Xin Y, Yin M, Zhao L, et al. Recent progress on nanoparticle-based drug delivery systems for cancer therapy. *Cancer Biol Med.* 2017; 14(3):111–241.
- [2] Din FU, Aman W, Ullah I, et al. Effective use of nanocarriers as drug delivery systems for the treatment of selected tumors. *Int J Nanomedicine.* 2017;12:7291–7309.
- [3] Cho K, Wang X, Nie S, et al. Therapeutic nanoparticles for drug delivery in cancer. *Clin Cancer Res.* 2008;14(5):1310–1316.
- [4] Deshpande PP, Biswas S, Torchilin VP. Current trends in the use of liposomes for tumor targeting. *Nanomedicine.* 2013;8(9):1509–1528.
- [5] Olusanya TOB, Ahmad RRH, Ibegbu DM, et al. Liposomal drug delivery systems and anticancer drugs. *Molecules.* 2018;23(4):907.
- [6] Dhanasekaran S, Chopra S. Getting a Handle on Smart Drug Delivery Systems – A Comprehensive View of Therapeutic Targeting Strategies. In: Sezer, AD, editor. *Smart Drug Delivery System* [Internet]. London: IntechOpen; 2016 [cited 2022 May 06]. Available from: <https://www.intechopen.com/chapters/49277> doi: 10.5772/61388
- [7] Morales-Cruz M, Delgado Y, Castillo B, et al. Smart targeting to improve cancer therapeutics. *Drug Des Dev Ther.* 2019;13: 3753–3772.
- [8] Jain A, Jain SK. Advances in tumor targeted liposomes. *Curr Mol Med.* 2018;18(1):44–57.
- [9] Golombek SK, May JN, Theek B, et al. Tumor targeting via EPR: strategies to enhance patient responses. *Adv Drug Deliv Rev.* 2018;130:17–38.
- [10] Huwyler J, Drewe J, Krähenbühl S. Tumor targeting using liposomal antineoplastic drugs. *Int J Nanomedicine.* 2008;3:21–29.
- [11] Riaz MK, Riaz MA, Zhang X, et al. Surface functionalization and targeting strategies of liposomes in solid tumor therapy: a review. *Int J Mol Sci.* 2018;19(1):195.
- [12] Immordino ML, Dosio F, Cattel L. Stealth liposomes: review of the basic science, rationale, and clinical applications, existing and potential. *Int J Nanomedicine.* 2006;1(3):297–315.
- [13] Noble GT, Stefanick JF, Ashley JD, et al. Ligand-targeted liposome design: challenges and fundamental considerations. *Trends Biotechnol.* 2014;32(1):32–45.
- [14] Sawant RR, Torchilin VP. Challenges in development of targeted liposomal therapeutics. *AAPS J.* 2012;14(2):303–315.
- [15] Marelli UK, Rechenmacher F, Sobahi A, et al. H. Tumor targeting via integrin ligands. *Front Oncol.* 2013;3:222.
- [16] Goodman SL, Picard M. Integrins as therapeutic targets. *Trends Pharmacol Sci.* 2012;33:405–412.
- [17] Desgrosellier JS, Cheresch DA. Integrins in cancer: Biological implications and therapeutic opportunities. *Nat Rev Cancer.* 2010;10:9–22.
- [18] Wang F, Li Y, Shen Y, et al. The functions and applications of RGD in tumor therapy and tissue engineering. *Int J Mol Sci.* 2013;14: 13447–13462.
- [19] Nieberler M, Reuning U, Reichart F, et al. Exploring the role of RGD-recognizing integrins in cancer. *Cancers.* 2017;9:116.
- [20] Sun C-C, Qu X-J, Gao Z-H. Arginine-glycine-aspartate-binding integrins as therapeutic and diagnostic targets. *Am J Ther.* 2016; 23(1):e198–e207.
- [21] Schroeder A, Avnir Y, Weisman S, et al. Controlling liposomal drug release with low frequency ultrasound: mechanism and feasibility. *Langmuir.* 2007;23(7):4019–4025.
- [22] Schroeder A, Kost J, Barenholz Y. Ultrasound, liposomes, and drug delivery: principles for using ultrasound to control the release of drugs from liposomes. *Chem Phys Lipids.* 2009;162(1–2):1–16.
- [23] Mullick Chowdhury S, Lee T, Willmann JK. Ultrasound-guided drug delivery in cancer. *Ultrasonography.* 2017;36(3):171–184.
- [24] Torchilin VP, Weissig V. *Liposomes: a practical approach.* Oxford, Oxford University Press; 2003. p. 396. <http://www.tandfonline.com/toc/rwhi20/>.
- [25] Sharma A, El-Faham A, de la Torre BG, et al. Exploring the orthogonal chemoselectivity of 2,4,6-trichloro-1,3,5-triazine (TCT) as a trifunctional linker with different nucleophiles: rules of the game. *Front Chem.* 2018;6:516.
- [26] Manjappa AS. Design and characterization of immunoliposomes for site specific delivery of selected anticancer drug. India, University of Vadodara; 2012.
- [27] Awad NS, Paul V, Mahmoud MS, et al. Effect of pegylation and targeting moieties on the ultrasound-mediated drug release from liposomes. *ACS Biomater Sci Eng.* 2020;6(1):48–57.
- [28] Ishii F, Nagasaka Y. Simple and convenient method for estimation of marker entrapped in liposomes. *J Dispers Sci Technol.* 2007; 22(1):97–101.
- [29] Alsawafah NM. The use of transferrin and ultrasound in cancer treatment. Sharjah: American University of Sharjah; 2019.
- [30] Awad NS, Paul V, Al-Sayah MH, et al. Ultrasonically controlled albumin-conjugated liposomes for breast cancer therapy. *Artif Cells Nanomed Biotechnol.* 2019;47(1):705–714.
- [31] Staples BJ, Roeder BL, Husseini GA, et al. Role of frequency and mechanical index in ultrasonic-enhanced chemotherapy in rats. *Cancer Chemother Pharmacol.* 2009;64(3):593–600.
- [32] University of New South Wales. Acoustic impedance, intensity and power.
- [33] Husseini GA, Diaz de la Rosa MA, Richardson ES, et al. The role of cavitation in acoustically activated drug delivery. *J Control Release.* 2005;107(2):253–261.
- [34] Song Z, Lin Y, Zhang X, et al. Cyclic RGD peptide-modified liposomal drug delivery system for targeted oral apatinib administration: enhanced cellular uptake and improved therapeutic effects. *Int J Nanomedicine.* 2017;12:1941–1958.
- [35] Afadzi M, Davies C de L, Hansen YH, et al. Effect of ultrasound parameters on the release of liposomal calcein. *Ultrasound Med Biol.* 2012;38(3):476–486.
- [36] Cohen-Levi D, Kost J, Barenholz Y. *Ultrasound for targeted delivery of cytotoxic drugs from liposomes.* Beer Sheva: Ben Gurion University; 2000.
- [37] Elamir A, Ajith S, Sawafah NA, et al. G. A. (2021). Ultrasound-triggered herceptin liposomes for breast cancer therapy. *Scientific reports,* 11(1):7545. doi: 10.1038/s41598-021-86860-5
- [38] Ben-Daya M, Paul V, Awad NS, et al. Targeting breast cancer using hyaluronic acid-conjugated liposomes triggered with ultrasound. *J Biomed Nanotechnol.* 2021;17(1):90–99.
- [39] Graham SM, Carlisle R, Choi JJ, et al. Inertial cavitation to non-invasively trigger and monitor intratumoral release of drug from intravenously delivered liposomes. *J Control Release.* 2014;178(1): 101–107.
- [40] Duco W, Grosso V, Zaccari D, et al. Generation of ROS mediated by mechanical waves (ultrasound) and its possible applications. *Methods.* 2016;109:141–148.
- [41] Frenkel V. Ultrasound mediated delivery of drugs and genes to solid tumors. *Adv Drug Deliv Rev.* 2008;60(10):1193–1208.
- [42] Stringham SB, Viskovska MA, Richardson ES, et al. Over-pressure suppresses ultrasonic-induced drug uptake. *Ultrasound Med Biol.* 2009;35(3):409–415.

- [43] Apfel RE, Holland CK. Gauging the likelihood of cavitation from short-pulse, low-duty cycle diagnostic ultrasound. *Ultrasound Med Biol.* 1991;17(2):179–185.
- [44] Şen T, Tüfekçioğlu O, Koza Y. Mechanical index. *Anatol J Cardiol.* 2015;15(4):334–336.
- [45] Meijering BDM, Juffermans LJM, van Wamel A, et al. Ultrasound and microbubble-targeted delivery of macromolecules is regulated by induction of endocytosis and pore formation. *Circ Res.* 2009;104(5):679–687.
- [46] Awad NS, Paul V, AlSawafthah NM, et al. Ultrasound-Responsive nanocarriers in cancer treatment: a review. *ACS Pharmacol Transl Sci.* 2021 Mar 3;4(2):589–612. doi: [10.1021/acsptsci.0c00212](https://doi.org/10.1021/acsptsci.0c00212). PMID: 33860189; PMCID: PMC8033618.
- [47] AlSawafthah NM, Awad NS, Paul V, et al. Transferrin-modified liposomes triggered with ultrasound to treat HeLa cells. *Sci Rep.* 2021;11(1):1–15.
- [48] Han SM, Na YG, Lee HS, et al. Improvement of cellular uptake of hydrophilic molecule, calcein, formulated by liposome. *J Pharm Investig.* 2018;48(5):595–601.
- [49] Vogel K, Wang S, Lee RJ, et al. Peptide-mediated release of folate-targeted liposome contents from endosomal compartments. *J Am Chem Soc.* 1996;118(7):1581–1586.
- [50] Jonker CTH, Deo C, Zager PJ, et al. Accurate measurement of fast endocytic recycling kinetics in real time. *J Cell Sci.* 2020 Jan 22; 133(2):jcs.231225. doi: [10.1242/jcs.231225](https://doi.org/10.1242/jcs.231225). PMID: 31843759; PMCID: PMC6983720.
- [51] Feng C, Li X, Dong C, et al. Rgd-modified liposomes enhance efficiency of aclacinomycin a delivery: evaluation of their effect in lung cancer. *Drug Des Devel Ther.* 2015;9:4613–4620.
- [52] Zhou X, Liu HY, Zhao H, et al. RGD-modified nanoliposomes containing quercetin for lung cancer targeted treatment. *Onco Targets Ther.* 2018;11:5397–5405.
- [53] Vakhshiteh F, Khabazian E, Atyabi F, et al. Peptide-conjugated liposomes for targeted miR-34a delivery to suppress breast cancer and cancer stem-like population. *J Drug Deliv Sci Technol.* 2020; 57:101687.
- [54] Aryal M, Vykhodtseva N, Zhang YZ, et al. Multiple treatments with liposomal doxorubicin and ultrasound-induced disruption of blood-tumor and blood-brain barriers improve outcomes in a rat glioma model. *J Control Release.* 2013;169(1–2):103–111.
- [55] Yang F-Y, Wong T-T, Teng M-C, et al. Focused ultrasound and interleukin-4 receptor-targeted liposomal doxorubicin for enhanced targeted drug delivery and antitumor effect in glioblastoma multi-forme. *J Control Release.* 2012;160(3):652–658. Internet